

# Development of Micromechanics-Based Constitutive Model for Alumina Using Unified Mechanics Theory-Role of Micro-Cracks in Damage

Brahmadathan V.B.\* and Lakshmana Rao C.

*Department of Applied Mechanics and Biomedical Engineering, IIT Madras, Chennai - 600 036*

*\*E-mail: am19d024@smail.iitm.ac.in*

## ABSTRACT

Ceramic materials used in mechanical applications show variations in their properties due to the difference in the presence of cracks and various defects. The micro-crack length, orientation, geometry and wing crack formation and propagation within the ceramic material define the strength of the ceramic material. In this study, a micromechanics-based model that accounts for micro-cracks is developed. Unlike other micromechanics-based models, the current model defines failure based on entropy. Entropy generated with various micro-crack lengths, orientations and wing crack extensions is calculated using the energy approach. The Unified Mechanics Theory (UMT) is used to define the damage in the ceramic material, which can include all possible failure mechanisms. A representative volume element (RVE) with a pre-existing flaw is simulated to generate stress-strain curves. The effect of different initial crack lengths and orientations on alumina peak strength is also investigated.

**Keywords:** Ceramic material; Constitutive modeling; Unified Mechanics Theory (UMT)

## 1. INTRODUCTION

Ceramic materials have superior properties like high specific strength, hardness, thermal resistance, etc. So, it can be used in many applications, such as structural applications, impact-related applications, thermal coatings, etc.<sup>1-3</sup> Quasi-static and dynamic behaviour of these depends on parameters like confinement pressure, nature of loading, constituents used in the manufacture, the microstructure, etc. The samples of such material's strength and other properties have significant variations even if they are manufactured or processed similarly. It is due to the deviation of the distribution of cracks and other defects in the material. The mechanical behaviour also depends on the crack geometry, orientation, length, etc. Therefore, modelling ceramic material based on micromechanics is essential.

The material models used for numerical analysis can be broadly classified as phenomenological and micromechanical. The most common models under the first category are the Johnson-Holmquist series model<sup>4-5</sup>. These are empirical models and consist of many parameters that require experimental data. The limitation of the phenomenological model is that it does not consider the micro-mechanisms of the material deformation, and it requires much experimental data to define the constants. Micromechanical models in various literature are mainly based on the fracture mechanics approach and consider various micro-mechanisms of deformation and damage in the material. Addressio and Johnson's<sup>6</sup> model identifies the elastic and inelastic deformation based on the damaged surface, which depends on pressure and crack length. This model considers

the failure based on the critical crack density. The material model is compared with planar impact experiments of silicon carbide, boron carbide, and titanium diboride. In Rajendran's study<sup>7</sup>, they looked at how micro-cracks propagate when the applied strain energy exceeds a critical level. They used the effective strain energy release rate, considering two cases: one for mode I fracture and the other for mode I and II fracture. The model also accounted for pulverised ceramic behaviour using the Mohr-Coulomb law. In this model, damage in the material is defined based on the density of cracks, and the material fails when this density reaches a specific limit: the shear and bulk moduli of the material decrease as the crack density increases. Ravichandran and Subhash's<sup>8</sup> model is based on a single crack without crack interaction effect. Failure occurs at the crack density reaches the critical crack density. This model is validated with experimental values of the dynamic strength of Aluminium Nitride.

Paliwal and Ramesh<sup>9</sup> used the sliding flaw model to develop the constitutive model. Crack-matrix-effective-medium model is used for incorporating interaction between the cracks. Probability distribution functions (pdf) represent the distribution of the flaw geometry. The frictional sliding of the crack surfaces causes inelastic deformation. The damage was caused by the crack nucleation and opening of the wing crack. In this model, the crack density parameter depends on the pdf, flaw size and increment in the wing crack length. A phenomenological form of crack-growth law is used in this model. Katcoff and Graham-Brady<sup>10</sup> followed the framework of Paliwal and Ramesh, and this model considers the crack growth from circular pores and slit-like flaws. The micro-mechanical model developed by Deshpande and Evans<sup>11</sup> considers micro-cracking

and plasticity due to dislocation motion depending on the confining pressure. Damage is defined based on wing crack length increment due to frictional sliding of the initial flaw surfaces. A single orientation of the initial crack is considered in this model. An extended version of the Deshpande Evans model is used to study the indentation of Corbit 98 ceramic<sup>12</sup>. These micromechanical models consider micro-cracking as the primary failure mechanism. Some models consider plasticity at high confinement pressure and the commutated material's granular behaviour. S.K Lahiri et al.<sup>13</sup> compared different constitutive models, such as the Johnson-Holmquist series and Deshpande-Evans models. They reported that the Deshpande-Evans model could not capture the mechanical response at a higher velocity. Damage defined in the existing models is mainly based on the crack density, which changes with the wing crack length. But there are other mechanisms which govern the deformation of Alumina<sup>14-15</sup>.

In this study, damage is characterised by quantifying the entropy produced during deformation. Utilising entropy to define damage offers a key advantage because it can encompass a wide range of deformation and failure mechanisms. The Unified Mechanics Theory (UMT) can incorporate various mechanisms that cause damage into a single thermodynamic state index (TSI) parameter, achieved by computing entropy throughout the deformation process<sup>16</sup>. The extent of damage in the material can be represented using this TSI parameter, which ranges from zero for an undamaged reference material to one for a wholly failed material. TSI is derived from the entropy generated within the material due to energy dissipation. Entropy is assessed based on the energy lost due to numerous internal processes within the material that ultimately lead to failure. UMT-based constitutive models are successfully implemented for metals and composites for various types of loading<sup>17-19</sup>, but applying UMT in modelling brittle material like Alumina is the least studied. A representative volume element technique is used in the current work to calculate entropy and TSI from the energy-dissipating micro-cracking mechanism; including other possible mechanisms<sup>15</sup> will be the future part of the work.

The objectives of the paper are:

- To utilise Unified Mechanics Theory for developing a micro-mechanical constitutive model for Alumina by considering the effect of pre-existing crack's length and orientation.
- To predict the stress-strain response of Alumina using UMT for all possible configurations of micro-crack lengths and orientations.

The article is organised as follows. First, the paper discusses the Unified Mechanics Theory. Then, details about the micromechanical model, RVE, and boundary condition. The following section discusses the procedure to calculate entropy and TSI for different orientations and lengths of the micro-crack. Finally, the constitutive model and stress-strain curve for Alumina and other significant results are discussed.

**2. UNIFIED MECHANICS THEORY**

Unified Mechanics Theory combines Newton's universal laws of motion and thermodynamics' first and second laws<sup>16</sup>.

According to UMT, material degradation can be evaluated based on the Thermodynamic State Index (TSI), which varies from zero to one. The modified laws of motion based on UMT are;

The second law of UMT,

$$F(1-\phi)dt=d(mv) \tag{1}$$

where F, m and v are force, mass and velocity.

The third law of UMT, Reaction force due to the application of load, reduces with time because the stiffness degrades with time.

$$\text{Applied force, } F_{12}=k_{21}u_{21}(1-\phi) \tag{2}$$

Thermodynamic State Index (TSI),

$$\Phi = \left[ 1 - e^{-\frac{m_s \Delta s}{R}} \right] \tag{3}$$

where,  $k_{21}$  and  $u_{21}$  are the stiffness and displacement of the reacting system.  $m_s$ ,  $\Delta s$ , and R molar mass, entropy and gas constant.

**3. MICRO-MECHANICAL MODEL**

A micro-mechanical model considers the mechanism of deformation and failure, which gives more insight into the material's behaviour. Various defects (for example, cracks, pores, etc.) can initiate failure in the ceramic material during deformation. This study considers a micro-mechanical model incorporating Alumina's micro-structure for developing the constitutive model. The current model considers crack propagation from these pre-existing cracks, which causes the material failure. The crack length and its orientation also affect the material behaviour. A representative volume element approach is used in this study to incorporate the micro-mechanism of deformation and failure.

**3.1 Representative Volume Element (RVE)**

A representative volume element with a pre-existing crack is considered to develop the constitutive model. A Finite Element model was created with periodic boundary conditions. Using Abaqus/standard software, numerical simulations were performed to find the energy required for the crack extension for different initial micro-crack lengths and orientations. Linear triangular elements are used for the simulations with fine mesh near the crack (2 μm) and coarse mesh towards the boundary.

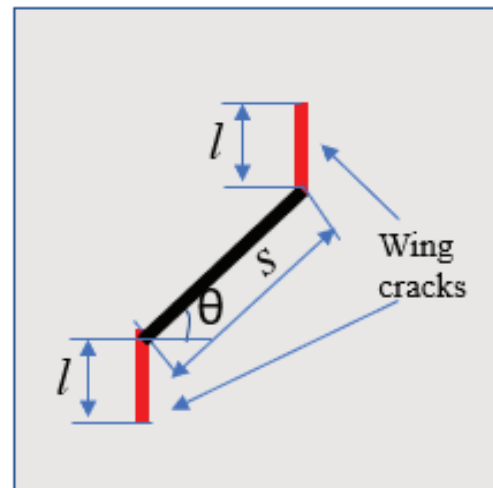


Figure 1. RVE with initial crack and wing crack.

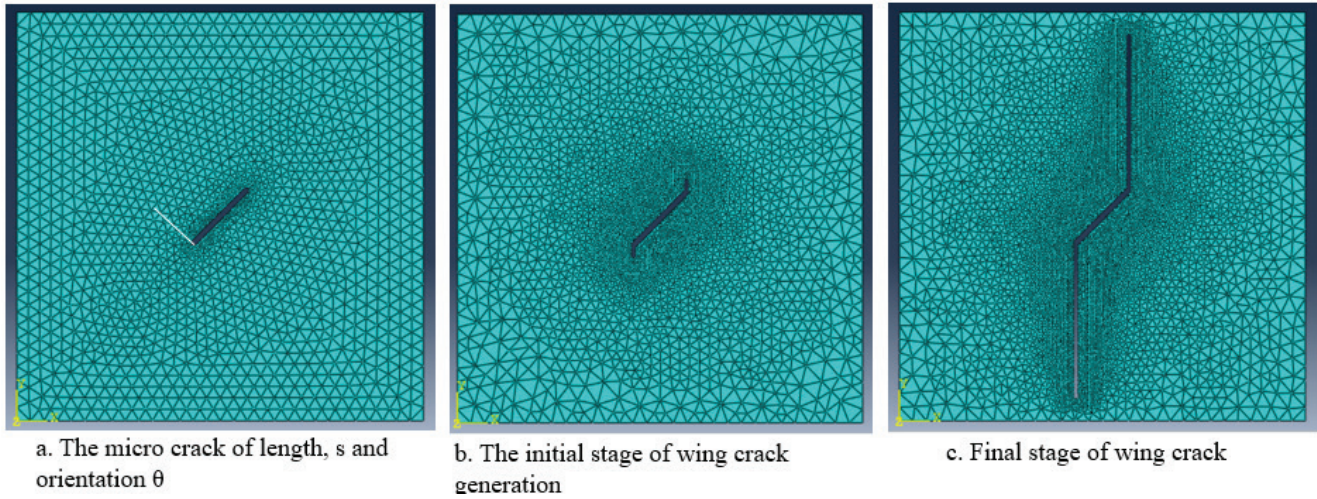


Figure 2. Initial stage of RVE to final stage during the crack propagation.

Under compressive load, the initial micro-crack surface slides each other, and it causes the formation of a wing crack from the tip of the initial micro crack. As the applied load increases, the wing crack length increases, and finally, it causes the failure of the material. The properties of Alumina used for the simulations (Table 1), and the size of RVE (200x200  $\mu\text{m}$ ) and initial micro-crack length were chosen according to the grain size of Alumina. The initial micro-crack lengths are 30, 40, 50 and 60  $\mu\text{m}$ , with different orientations of 30, 45, 60 and 75 degrees considered in this study. The strain energy required for each wing crack length increment is calculated from the force-deflection curve of each RVE.

Table 1. Mechanical properties of Alumina

Elastic modulus, E	380 GPa
Poisson's ratio	0.24
Grain size[20]	20 $\mu\text{m}$
Tensile strength[20]	200 MPa
Mode I Stress intensity factor[21]	3.8-5.1 $\text{MNm}^{-3/2}$

### 3.2 Boundary Conditions

The boundary condition used for the RVE is shown in the figure. Periodic boundary conditions (PBC) are used to get homogeneous behaviour of the material for different combinations of initial micro-crack length and orientations.

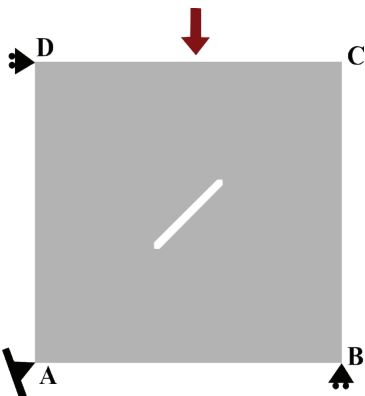


Figure 3. Representative volume element with periodic boundary condition.

The periodic boundary condition is implemented using the following Eqn.;

Edge nodes:

$$u^{CB} - u^{AD} - \Delta x \varepsilon_{xx} = 0 \quad (4.a)$$

$$v^{CB} - v^{AD} = 0 \quad (4.b)$$

$$v^{DC} - v^{AB} - \Delta y \varepsilon_{yy} = 0 \quad (4.c)$$

$$u^{DC} - u^{AB} = 0 \quad (4.d)$$

Corner nodes:

$$u^C - u^D - \Delta x \varepsilon_{xx} = 0 \quad (5.a)$$

$$v^C - v^D = 0 \quad (5.b)$$

$$v^C - v^B - \Delta y \varepsilon_{yy} = 0 \quad (5.c)$$

$$u^C - u^B = 0 \quad (5.d)$$

where,  $u$  and  $v$  are displacements in the  $x$  and  $y$  direction,  $\Delta x$  and  $\Delta y$  are the RVE size.

$\varepsilon_{xx}$  and  $\varepsilon_{yy}$  are strains in the  $x$  and  $y$  direction.

### 4. ESTIMATION OF ENTROPY AND TSI

Entropy is generated during the deformation of the material if there is a dissipation of energy. Under compressive loading of Alumina, during the initial stage, the applied energy is used for the deformation of the material, and the force applied to the material may not be enough to propagate the pre-existing crack. Rankine criteria for brittle material are used as the crack propagation criteria in the study. As the applied load increases, the stress near the crack tip increases; if the crack tip stress exceeds the material's tensile strength, the wing crack generates and will propagate. Since the fracture in brittle material from the initial crack occurs through sliding and opening deformation (mixed mode), stress-based fracture criteria such as Rankine criteria can be used as the crack propagation criteria. As the crack propagates from the initial micro-crack, there is a combination of an inclined initial crack and a wing crack, which propagates parallel to the applied load. In this situation, FE simulation helps to find the stress near the crack tip, which doesn't require the values of the mode I and mode II stress intensity factors. The energy required for crack propagation is the energy dissipated during the deformation.

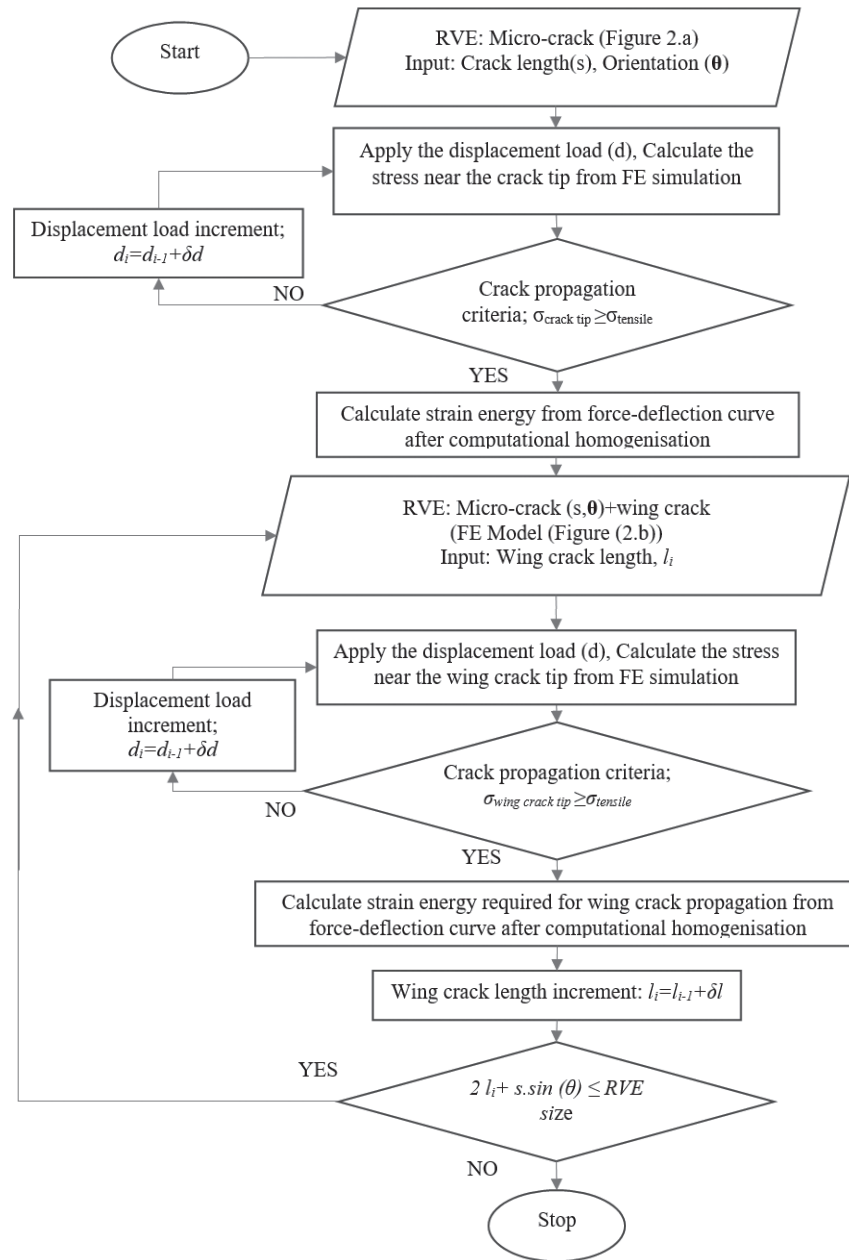


Figure 4. Methodology used in FE simulation.

Therefore, the entropy generated during the crack propagation can be calculated by Eqn. 6.

$$\Delta S = \frac{\text{Change in entropy, } \Delta U_{\text{crack extension}}}{\rho T} = \frac{U_1 - U_{1+\Delta l}}{\rho T} \quad (6)$$

where, U= Strain energy  
 l=crack length  
 Δl=Wing crack length increment

Strain energy is computed initially for a specific micro-crack length (s) and orientation (θ) by analysing the force-deflection response until crack propagation occurs. Once the crack propagation starts with the same s and θ, a wing crack of length l is introduced into a different finite element (FE) model (Fig. 2. b). A new FE model is created, considering an increased wing crack length (l+δl) when the crack propagation criteria

have been met in the previous FE model. This iterative process is repeated until the wing crack extends to the Representative Volume Element (RVE) boundary, as illustrated in Fig. 2(c). The Thermodynamic State Index (TSI) and entropy can be determined based on the energy required for the wing crack propagation. This procedure is replicated for all feasible combinations of initial crack length (s) and orientation (θ) (Fig. 4).

### 5. CONSTITUTIVE MODELS FOR ALUMINA

The micro-mechanical model considered in this work consists of slit-like flaws. The main goal of this model is to generate a stress-strain curve for brittle materials such as Alumina under low strain rate compressive loading conditions.

Three different constitutive models are presented here: (1) A micromechanical model developed by Paliwal-Ramesh[9]

for ceramic material, it is used to validate other two models; (2) FEM-UMT-based constitutive model; (3) UMT-based model in which TSI replaces damage defined in the Paliwal-Ramesh model.

### 5.1 Paliwal-Ramesh Model<sup>9</sup>

The constitutive Eqn. are;

$$\sigma = E_{eff} \varepsilon \quad (7)$$

Effective stress acting on the crack,

$$\tau_{eff} = \tau_c - \mu(\sigma_{11}^{local} \cos^2 \theta + \sigma_{22}^{local} \sin^2 \theta + \sigma_{12}^{local} \sin 2\theta) + \left( \frac{1}{2} (\sigma_{11}^{local} - \sigma_{22}^{local}) \sin 2\theta - \sigma_{12}^{local} \cos 2\theta \right) \quad (8)$$

Stress intensity factor at the crack tip,

$$K_I = \frac{-2s \tau_{eff} \cos(\theta)}{\sqrt{2\pi(l+0.27s)}} + \sigma_{22}^{local} \sqrt{\pi l} \quad (9)$$

$$\text{Crack growth criteria: Stress Intensity factor, } K_I = K_{IC} \quad (10)$$

Crack growth rate,

$$\dot{l} = \frac{C_R}{\alpha} \left( \frac{K_I - K_{IC}}{K_I - 0.5K_{IC}} \right)^Y \quad (11)$$

Damage evolution,

$$\dot{D} = 2\eta \sum_{j=1}^N g(s) \Delta s l_j \dot{l}_j \quad (12)$$

Effective modulus<sup>22</sup>,

$$E_{eff} = E \left( 1 - \frac{\pi^2}{30} (1 + \nu)(5 - 4\nu)D \right) \quad (13)$$

$\theta$ ,  $s$ , and  $l$  are Crack orientation, initial crack length and wing crack length

$\mu$  and  $\tau_c$  are the coefficients of dry friction and cohesion.

$\sigma_{11}^{local}$ ,  $\sigma_{22}^{local}$  and  $\sigma_{12}^{local}$  are the stresses in the elliptical inclusion, which contains the crack; this is used to include the effect of interaction between the crack.

$K_{IC}$ =Critical stress intensity factor.  $C_R$ = Rayleigh wave velocity;  $\alpha$  and  $\gamma$  are constants.

$\eta$  is the crack density.  $g(s)$  is the probability distribution function.  $E$  and  $\nu$  are the modulus of elasticity and Poisson's ratio.

### 5.2 FEM-UMT-Based Constitutive Model

An overview of the FEM-UMT-based constitutive model is illustrated in Fig. 5. For simplicity, the Rankine type criterion is used as the crack propagation criteria suited for brittle materials. When the crack propagation criteria are satisfied for a particular initial micro-crack length and orientation, wing cracks are introduced in the FE model. The strain energy required for the crack propagation is taken from the FE simulation data to estimate the entropy generated for each wing crack length. A Bi-variate probability density function (PDF) of exponential form is used to incorporate all possible combinations of initial crack length and orientation.

The damage is defined based on the crack density in the Paliwal-Ramesh constitutive model, and the FEM-UMT-based model uses entropy to determine the damage.

### 5.3 UMT-based Model

The micromechanical model developed by the Paliwal-Ramesh Model can be modified by replacing the crack density-based damage with entropy and TSI.

Therefore, the damage is defined using the thermodynamic state index, TSI (Eqn. 3). For this, energy dissipated during the crack propagation is required.

The stress intensity factor calculated from Eqn.6 calculates the strain energy release rate.

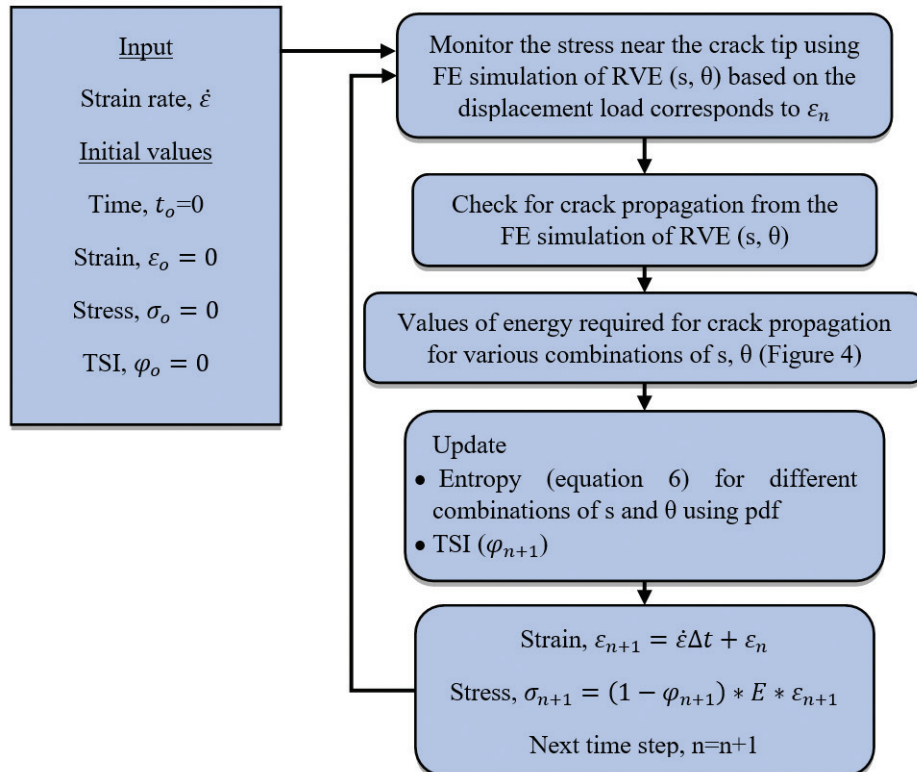


Figure 5. Overview of the FEM-UMT constitutive model.

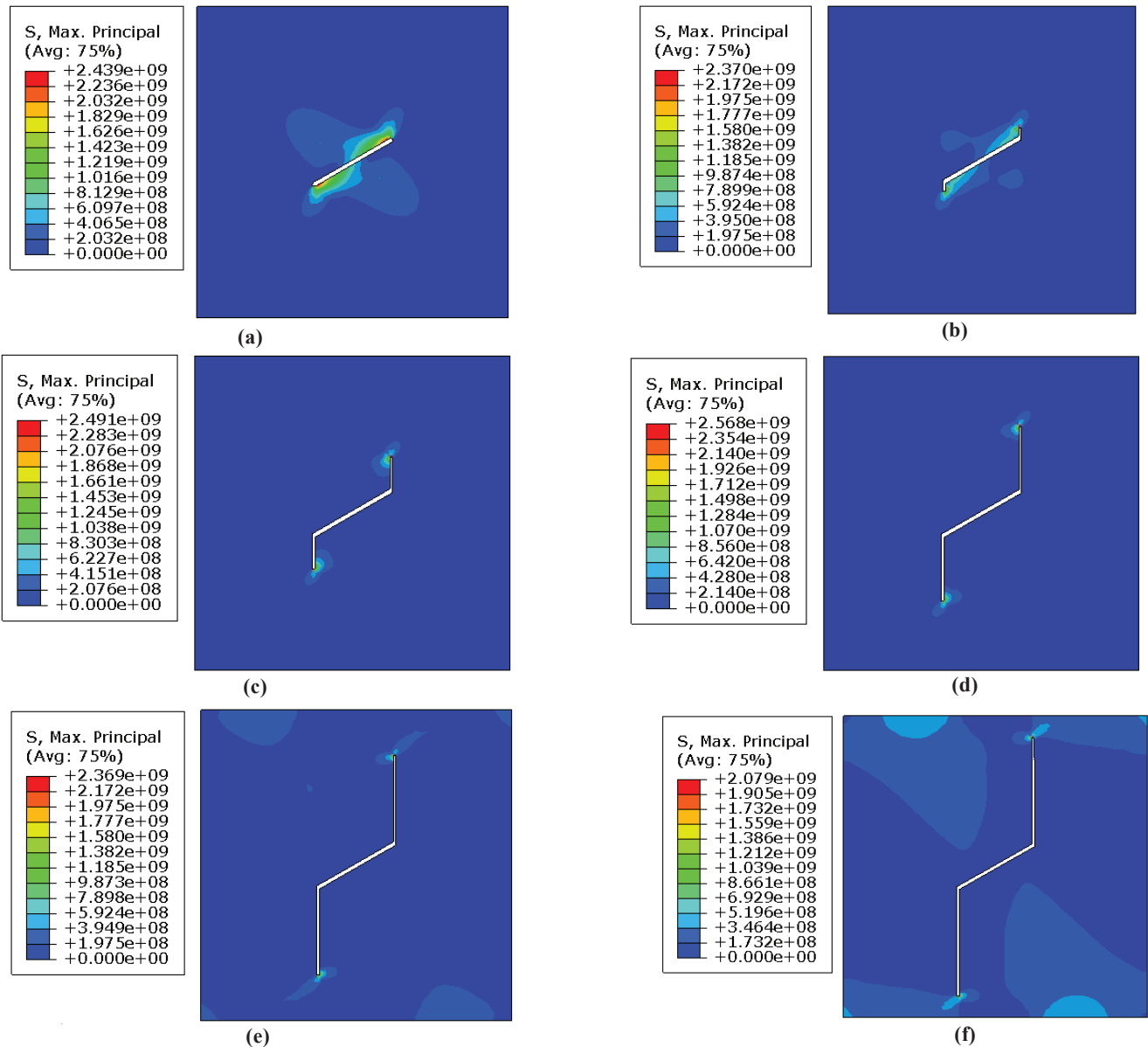


Figure 6. Various stages of crack propagation, (a) Initial Micro-crack of 60  $\mu\text{m}$  and orientation of 30°; (b) Micro-crack and wing crack (5  $\mu\text{m}$ ); (c) Micro-crack and wing crack (20  $\mu\text{m}$ ); (d) Micro-crack and wing crack (40  $\mu\text{m}$ ); (e) Micro-crack and wing crack (55  $\mu\text{m}$ ); and (f) Micro-crack and wing crack (70  $\mu\text{m}$ ).

$$G = \frac{K_I^2}{E} \quad (14)$$

Strain energy required for the crack propagation,  
 $SE = G l$  (15)

Entropy generated for the crack propagation,  $s = \frac{SE}{\rho T}$  (16)

where,  $\rho$  and  $T$  are density and temperature

Using Eqn. 3, the TSI evolution can be found, and effective modulus can be expressed in terms of TSI.

$$E_{eff} = E(1 - \Phi) \quad (17)$$

## 6. RESULTS AND DISCUSSIONS

FEM simulations for an initial micro-crack length of 60  $\mu\text{m}$  and orientation of 30° are shown in Fig. 6.

The entropy and TSI of RVE are calculated from the FE simulations using Eqns.3 and 6. The estimated entropy and TSI

for initial micro-crack lengths of 30  $\mu\text{m}$  to 60  $\mu\text{m}$  with different orientations are shown in Fig.7. Entropy generation increases with an increase in wing crack length. Similar data for other combinations of micro-crack length and orientations were obtained using the FEM simulation of RVE.

The stress-strain curve for a single micro-crack was generated for the FEM-UMT-based model, and the results are compared with the Paliwal-Ramesh model. The input values for the Paliwal-Ramesh model are  $\alpha=1$ ,  $\gamma=1$ , critical stress intensity factor,  $K_{IC}=5 \text{ MNm}^{-3/2}$  and  $\tau_c=0$ . The stress-strain response of Alumina using the three models for quasi-static uniaxial compressive load is shown in Figure 8 (Initial crack length 60  $\mu\text{m}$  and orientation 30°). The three models' peak stress values yield similar results (Fig. 9).

Peak stress values and corresponding strain values match for Alumina at uniaxial compressive load with a strain rate of

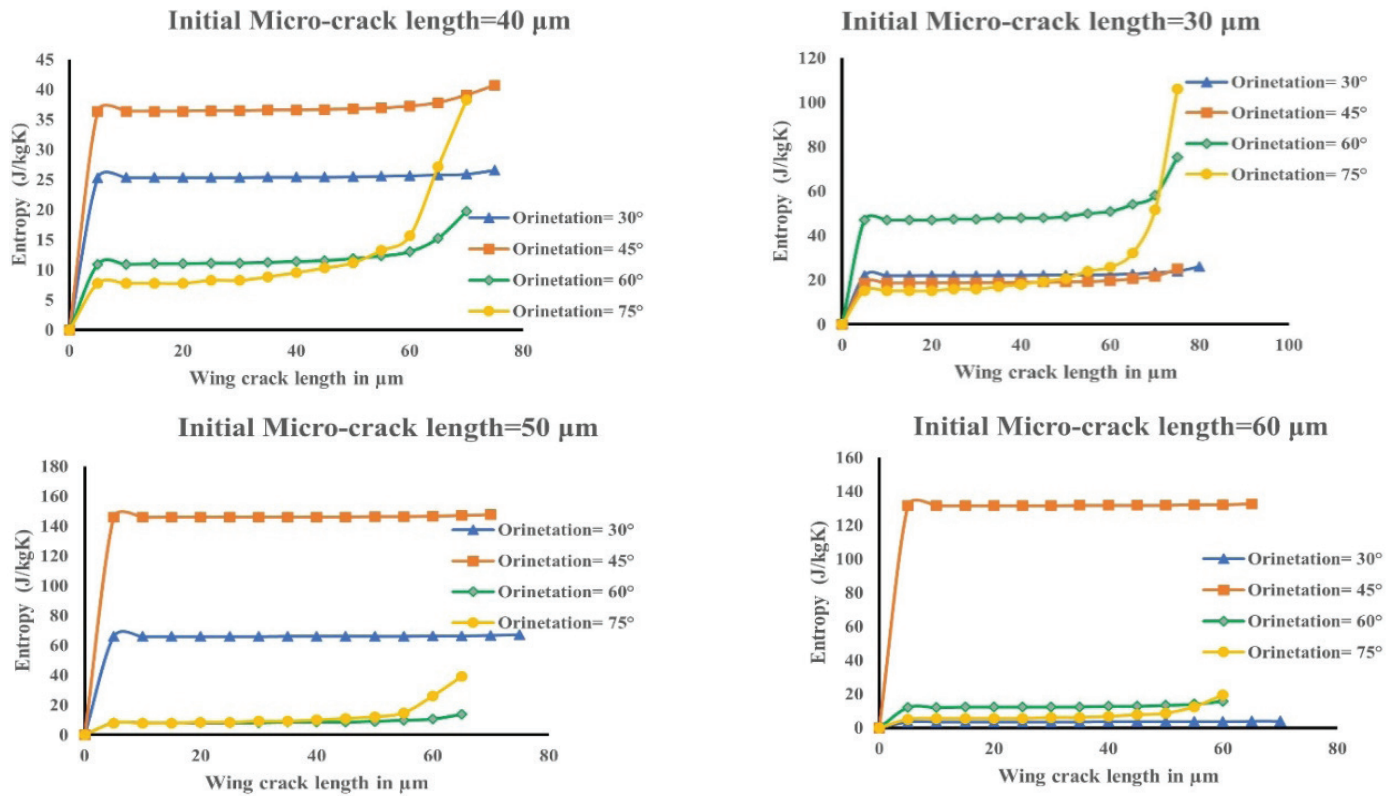


Figure 7. Entropy variation with wing crack length for different initial micro-crack length.

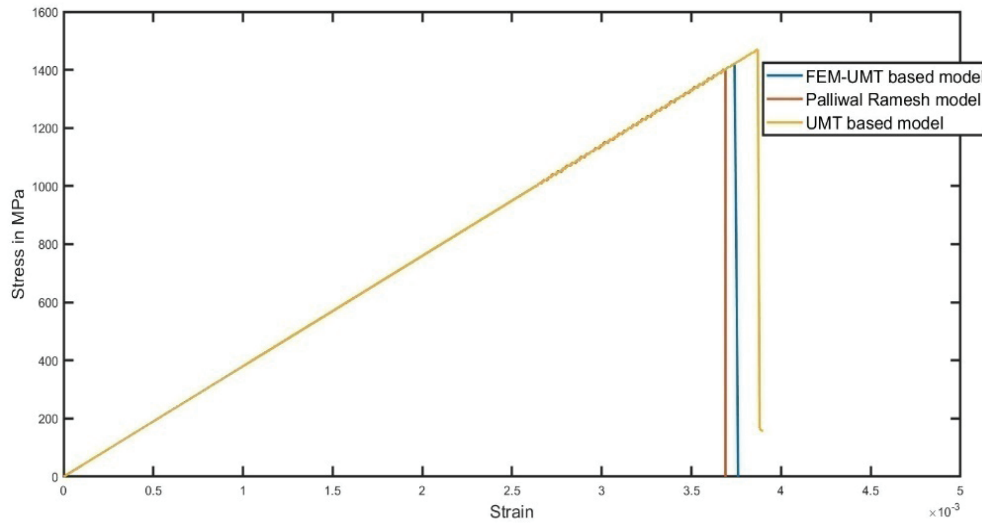


Figure 8. Stress-curve for three different models.

$1 \text{ s}^{-1}$ ; therefore FEM-UMT-based model can be used for all combinations of crack length and orientation.

The effect of all crack lengths and orientations can be incorporated into the constitutive model by including the probability distribution function. A bivariate probability distribution function of exponential form is used in this study, which consists of the effect of both crack length and orientation. The crack density of  $10^7 \text{ m}^{-2}$  is considered for the analysis.

The peak stress obtained by considering the combinations of micro-crack length and direction for the Paliwal-Ramesh model is 1401.14 MPa (strain=0.0036), the peak stress for the FEM-UMT based model is 1425.09 MPa (strain=0.00375),

and the peak stress for the modified Paliwal-Ramesh model with new damage definition based on entropy (TSI) is 1402.2 MPa (strain=0.00369) (Fig. 10). Therefore, The FEM-UMT-based model can predict the response of the alumina ceramics with TSI as the damage metric.

A multiscale modelling approach is employed in this study, utilising finite element (FE) simulations of a Representative Volume Element (RVE) containing pre-existing flaws. Computational homogenisation is used to determine the macroscopic material properties. This method is an efficient means of quantifying the energy dissipated during crack propagation. The FE model can be improved

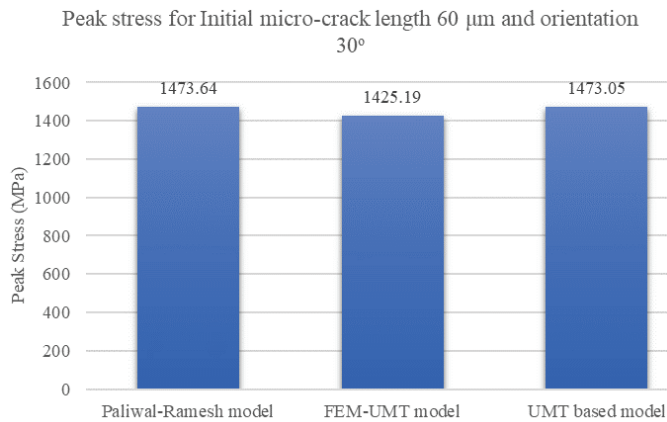


**Figure 9. Peak Stress values of three different models (One combination of crack length and orientation).**

by adding grains around the pre-existing crack and assigning grain-level anisotropic properties to each grain. The energy dissipation during crack propagation serves as the measure of damage in ceramics, as defined by the thermodynamic state index (TSI), derived from the principles of the second law of thermodynamics. Consequently, the developed model adheres to thermodynamic principles, ensuring thermodynamic consistency. Entropy-based damage (TSI) can accommodate various energy-dissipating mechanisms in ceramic material deformation, such as crack nucleation, crack branching, plastic deformation at high confining pressure, etc. In contrast, non-entropy-based damage definitions rely on observable field variables like crack area or density, but they cannot encompass other dissipative mechanisms within the same damage definition. Conversely, entropy-based damage assessment through TSI can account for damage caused by various potential energy-dissipating mechanisms. The focus of future research is the evaluation of TSI based on multiple energy dissipating mechanisms and including strain rate effect in the model.

## 7. CONCLUSIONS

A micromechanical model for Alumina is developed by considering micro-cracking as the energy-dissipating mechanism. The damage evolution due to the crack propagation is defined based on entropy generation and TSI.

FE-based RVE is used to evaluate the entropy and TSI for ceramic material. Stresses near the crack tip are monitored, and Rankine criteria are used for the crack propagation in the FEM-UMT model.

The values of TSI change from zero to one, and the mechanism considered here for entropy generation is crack propagation from pre-existing micro-cracks of different lengths and orientations.

The developed model is compared with the existing micro-mechanical model (Paliwal-Ramesh model) by using stress-stress response at a strain rate of  $1 \text{ s}^{-1}$  for the same input parameters such as initial crack density, configurations of crack length and orientation. The FEM-UMT-based model gives a peak stress value of 1425.09 MPa, peak stress value for the Paliwal-Ramesh model is 1401.14 MPa. Furthermore, the Paliwal-Ramesh model was modified by replacing crack length-based damage with entropy-based TSI, yielding

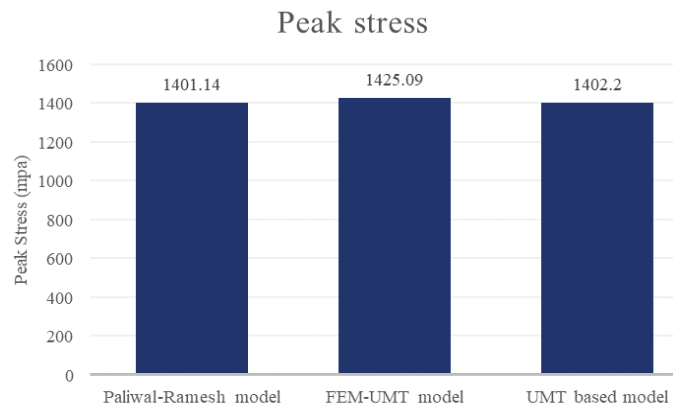


**Figure 10. Peak stress values of three different models.**

similar results. Therefore, a constitutive model in which TSI as a damage metric can predict the strength and stress-strain response of the alumina ceramics.

Including other dissipative mechanisms, such as crack nucleation and its propagation, micro-plasticity, and other possible mechanisms in the TSI evaluation will help in the complete formulation of ceramic material behaviour.

## REFERENCES

- Walley, S.M. Historical review of high strain rate and shock properties of ceramics relevant to their application in armour. *Adv. Appl. Ceramics*, 2010, **109**(8), 446–466. doi: 10.1179/174367609X422180.
- Forquin, P. Brittle materials at high-loading rates: An open area of research. *Philos. Transact. Royal Soc. A: Mathematical, Physical and Eng. Sci.*, 2017, **375**(2085). doi: 10.1098/rsta.2016.0436.
- Crouch, I.G. Body armour – New materials, new systems. *Defence Technology*. 2019, **15**(3), 241–253. doi: 10.1016/j.dt.2019.02.002.
- Johnson, G.R. & Holmquist, T.J. An improved computational constitutive model for brittle materials. *AIP Conf. Proc.*, May 2008, **309**(1), 981. doi: 10.1063/1.46199.
- Holmquist, T.J.; Johnson, G.R. & Gerlach, C.A. An improved computational constitutive model for glass. *Philos. Transact. Royal Soc. A: Mathematical, Physical and Eng. Sc.*, 2017, **375**(2085). doi: 10.1098/rsta.2016.0182.
- Addressio, F.L. & Johnson, J.N. A constitutive model for the dynamic response of brittle materials. *J. Appl. Phys.*, 1990, **67**(7), 3275–3286. doi: 10.1063/1.346090.
- Rajendran, A.M. Modeling the impact behavior of AD85 ceramic under multiaxial loading. *Int. J. Impact Eng.*, 1994, **15**(6), 749–768. doi: 10.1016/0734-743X(94)90033-H.
- Ravichandran, G. & Subhash, G. A micromechanical model for high strain rate behavior of ceramics. *Int. J. Solids Struct.*, 1995, **32**(17-18), 2627–2646. doi: 10.1016/0020-7683(94)00286-6.
- Paliwal, B. & Ramesh, K.T. An interacting micro-crack

- damage model for failure of brittle materials under compression. *J. Mech. Phys. Solids*, 2008, **56**(3), 896–923.  
doi: 10.1016/j.jmps.2007.06.012.
10. Katcoff, C.Z. & Graham-Brady, L.L. Modeling dynamic brittle behavior of materials with circular flaws or pores. *Int. J. Solids Struct.*, 2014, **51**(3–4), 754–766.  
doi: 10.1016/j.ijsolstr.2013.11.004.
  11. Deshpande, V.S. and Evans, A.G. Inelastic deformation and energy dissipation in ceramics: A mechanism-based constitutive model. *J. Mech. Phys. Solids*, 2008, **56**(10), 3077–3100.  
doi: 10.1016/j.jmps.2008.05.002.
  12. Gamble, E.A.; Compton, B.G.; Deshpande, V.S.; Evans, A.G. & Zok, F.W. Damage development in an armor ceramic under quasi-static indentation. *J. Am. Ceramic Soc.*, 2011, **94**(1), s215–s225.  
doi: 10.1111/j.1551-2916.2011.04472.x.
  13. Lahiri, S.K.; Shaw, A. & Ramachandra, L.S. On performance of different material models in predicting response of ceramics under high velocity impact. *Int. J. Solids Struct.*, 2019, 176–177, 96–107.  
doi: 10.1016/j.ijsolstr.2019.05.024.
  14. Lankford, J.; Predebon, W.W.; Staehler, J.M.; Subhash, G.; Pletka, B.J. & Anderson, C.E. The role of plasticity as a limiting factor in the compressive failure of high strength ceramics.
  15. Bhattacharya, M.; Dalui, S.; Dey, N.; Bysakh, S.; Ghosh, J. & Mukhopadhyay, A.K. Low strain rate compressive failure mechanism of coarse grain alumina. *Ceram. Int.*, 2016, **42**(8), 9875–9886.  
doi: 10.1016/j.ceramint.2016.03.087.
  16. Basaran, C. Introduction to unified mechanics theory with applications. *Introduction to Unified Mechanics Theory with Appl.*, 2021.  
doi: 10.1007/978-3-030-57772-8.
  17. Lee, H.W. & Basaran, C. A review of damage, void evolution, and fatigue life prediction models. *Metals (Basel)*, 2021, **11**(4), 2021.  
doi: 10.3390/met11040609.
  18. Lee, H.W. & Basaran, C. Predicting high cycle fatigue life with unified mechanics theory. *Mech. Mater.*, 2022, **164**, 104116.  
doi: 10.1016/j.mechmat.2021.104116.
  19. Basaran, C. & Nie, S. A thermodynamics based damage mechanics model for particulate composites. *Int. J. Solids Struct.*, 2007, **44**(3–4), 1099–1114.  
doi: 10.1016/j.ijsolstr.2006.06.001.
  20. Rice, R.W. Review ceramic tensile strength-grain size relations: Grain sizes, slopes, and branch intersections. *J. Mater. Sci.*, 1997, **32**, 1673–1692.
  21. Agrawal, D. C. Mechanical properties of alumina ceramics. *Transact. Indian Ceram. Soc.*, 1995, **54**(5), 185–189.  
doi: 10.1080/0371750X.1995.10804717.
  22. Budiansky, B. & O’Connell, R.J. Elastic moduli of a cracked solid. Pergamon Press, 1976.

## CONTRIBUTORS

**Mr Brahmadathan V.B.** is a Research Scholar at the Department of Applied Mechanics and Bio-Medical Engineering, IIT Madras. He obtained M.Tech in machine design from Kerala University. His areas of interest include constitutive modelling, finite element analysis, impact and fracture mechanics. He has contributed to conceptualisation, methodology, numerical simulations, original draft preparation, review & editing in this paper.

**Dr Lakshmana Rao** is a Professor in the Department of Applied Mechanics and Bio-medical Engineering at IIT Madras. He has obtained his bachelor’s and master’s degrees from the Department of Civil Engineering at IIT Madras and his DS in Mechanics of Materials from the Massachusetts Institute of Technology. His areas of specialisation include solid mechanics in general and damage mechanics, impact mechanics, fracture Mechanics and finite element analysis in particular. For this work, he contributed to the conceptualisation, methodology, review, editing, and supervision.